

A repeating earthquake catalog for the Atacama Segment in North Chile (24.5°S-30.5°S)

Jonas Folesky  * 1, Jörn Kummerow  1, Laurens Jan Hofman  1

¹Department of Geophysics, Freie Universität Berlin, Berlin, Germany

Author contributions: Conceptualization: J. Folesky, J. Kummerow. Methodology: L. J. Hofman, J. Folesky. Software: L. J. Hofman, J. Folesky. Formal Analysis: J. Folesky, L. J. Hofman. Writing - Original draft: J. Folesky. Writing - Review & Editing: J. Folesky, J. Kummerow. Visualization: J. Folesky. Funding acquisition: J. Folesky.

Abstract Repeating earthquakes are close to identical seismic events that recur on the same fault patch with consistent focal mechanisms. They can be used to estimate local fault slip and their magnitude-dependent recurrence intervals can serve to infer patterns of aseismically creeping zones at depth. We have constructed a long-term catalog of repeating earthquakes for the Atacama segment of the Chilean subduction zone. Using waveforms from approximately 60,000 earthquakes as templates, we performed GPU-based template matching on continuous data from 25 permanent seismic stations from 2014 to 2024 and one additional station with data from 1998 to 2024. The resulting catalog includes 4781 repeating events grouped into 1142 families, showing variability in size and behavior, from long-lasting sequences to short-term bursts. Several magnitude M 5.7+ earthquakes significantly influenced the occurrence rates of nearby repeaters. The dataset is dominated by the 2015 M_w 8.3 Illapel megathrust earthquake. This catalog aims to support detailed analysis of rupture processes, source structures, and the spatiotemporal evolution of slow slip at depth. The production and reporting style are similar to a previous article by Folesky et al. (2025) on the adjacent northern Chile repeater catalog.

Production Editor:
Yen Joe Tan
Handling Editor:
Mathilde Radiguet
Copy & Layout Editor:
Kirsty Bayliss

Received:
September 09, 2025
Accepted:
January 27, 2026
Published:
February 19, 2026

1 Introduction

The occurrence of repeating earthquakes (REs), or repeaters, has been well documented for many regions of the world and for various tectonic settings (cf. reviews by Uchida, 2019; Uchida and Bürgmann, 2019). They are conceived as seismic events which rupture repeatedly the same fault area, have nearly identical mechanisms and therefore exhibit highly similar waveforms (Menke, 1999). The prevalent model to explain repeaters is that of a close to identical, reiteratively activated slip patch of a strong asperity, which is surrounded by or adjacent to a region of aseismic creep, that consistently loads the locked asperity, enforcing repeated seismic energy release (e.g. Nadeau and Johnson, 1998; Matsuzawa et al., 2004; Chen et al., 2010). Therefore, repeaters are considered as tracers for the slip of their local aseismic environment at depth.

Identification of RE sequences (RES) is commonly achieved by computing the waveform cross correlation as a measure of waveform similarity (e.g. Igarashi et al., 2003). This is applied to search for similar events within an event catalog or by a template matching (also called match filter) technique, where the waveform of a given event is used as a template to search for similar events (matches) within the continuous seismic recordings. While repeaters are understood to represent ruptures of identical or at least overlapping patches of the same

fault, their practical identification is less well-defined. Hence, parameter thresholds and criteria for defining repeaters differ between authors (Gao et al., 2021).

In this work, we make use of the seismological recordings of the permanent stations available between 23°S and 32°S. The study region is strongly dominated by the subduction of the Nazca plate below the South American plate with an average velocity of 6.7 cm/yr. The very recent, local seismicity catalog of Münchmeyer et al. (2025) is used to extract template waveforms for \sim 60,000 events and then perform template matching for the continuous waveform data.

We identify over a thousand repeater series with a wide range of recurrence patterns and in different parts of the subduction zone. We label and classify them according to their location and variation of recurrence behavior, and we thereby aim to provide a solid basis for subsequent repeater based analysis in the future. In large parts, this work is a repetition of processing applied to the adjacent “Northern Chile” segment between 18°S and 24°S of the Chilean subduction zone by Folesky et al. (2025) and it complements this data set. The processing is customized only slightly for the Atacama Segment, especially for the years before 1998–2014, where only one station could be used for the catalog construction. The catalog is intended to serve as a basis for subsequent research, i.e., comparison to locking maps, swarm activity, slow slip phenomena, *et cetera*, as well as for comparison to repeater activity elsewhere.

*Corresponding author: jonas.folesky@geophysik.fu-berlin.de

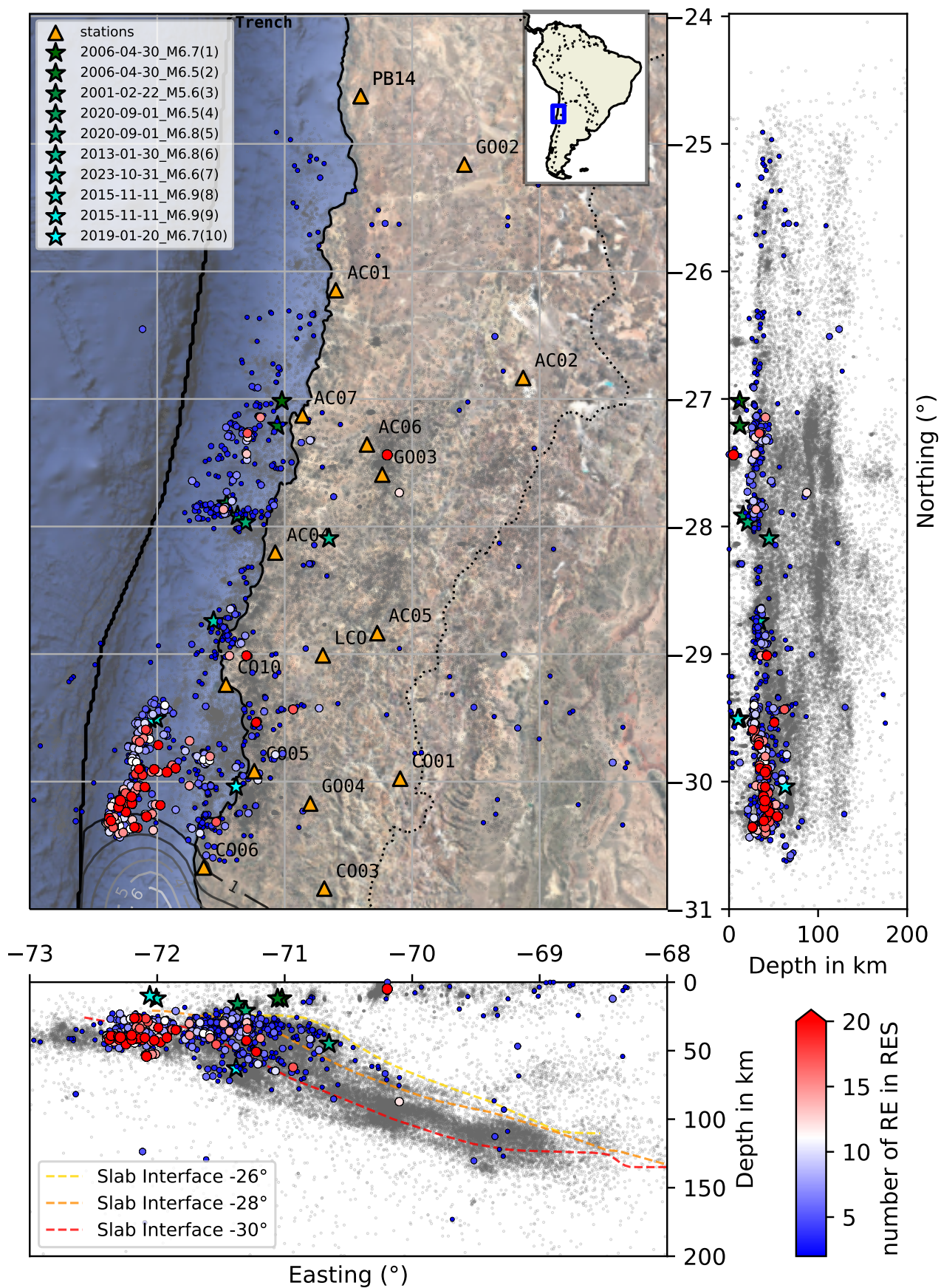


Figure 1 Repeating earthquake sequence (RES) locations in the target region. Color indicates the number of family members. Orange triangles are permanent seismic stations. The background seismicity, shown in gray, is taken from Münchmeyer et al. (2025), same as the slab geometry at different latitudes. In the south, the slip contours of the 2015 M_W 8.3 Illapel earthquake are shown (Ruiz et al., 2016). Its epicenter (origin: 2015-09-16 22:54:32, -31.57, -71.65, 22.4km (USGS)) is just outside of the map. Green to cyan stars show locations of selected large magnitude earthquakes in the study area, which affect repeater occurrences. Their sorting in the legend is from north to south. Locations stem from the USGS catalog.

2 Seismicity Data

This study is based on the seismological broadband data from the seismic CX network (4 stations, [IPOC \(2006\)](#)), the C1 network (17 stations, [\(C1, 2012\)](#)), the C network (3 stations, [\(C, 1991\)](#)), the IU network (1 stations, [\(IU, 1988\)](#)). All four networks provide publicly available continuous records from their permanent stations, accessible via [iris.edu](#) or [geofon.gfz.de](#). Here, we use the 40 Hz vertical component (BHZ) waveform data obtained by the broadband instruments from the permanent networks. The analyzed time period is from 2014 to 2024 for the C, C1, and CX nets, and late 1998 to 2024 for the station IU.LCO.

The recent Atacama segment seismicity catalog by [Münchmeyer et al. \(2025\)](#), which encompasses 60,374 events between 2014-05-01 and 2024-02-14, ranging from 24.5°S to 30.5°S, defines the template events for constructing the repeating earthquake catalog. Therefore, we limit the repeater catalog to the same area. Note, that the authors provide two versions of the catalog. We use the “permanent” version of the catalog. For detail please see [Münchmeyer et al. \(2025\)](#). Henceforth, we will call this seismicity catalog the Atacama seismicity catalog. An overview of the data availability for all stations can be found in the electronic supplement (Figure S1). Station locations are shown in Figure 1 & Figure S2.

3 Method

To search for repeating earthquakes in the entire continuous waveform data, we apply the template matching procedure described in [Hofman et al. \(2023\)](#) with principally the same specifications as in [Folesky et al. \(2025\)](#).

The chosen settings were as follows: For the template matching, recordings of all 60,374 earthquakes in the Atacama seismicity catalog were used as templates. The vertical component seismograms were extracted for each template at the five closest available stations, that have data. The length of the extracted time window was chosen variable, dependent on the source-receiver distance. Its minimum length was set to 15 s, and it was extended with hypocentral distance to ensure that the time window always contained both the P and S phases. Seismograms were 1-4 Hz band-pass filtered and down-sampled to 20 Hz to decrease computational costs.

For the definition of a match two different sets of thresholds were applied:

1. for the time interval of 1998-12-22 to 2014-05-01, where only one station was operational in the region, we require a minimum of cc=0.90 to define a match.
2. for the time period of 2014-05-01 to 2024-12-31 we require a minimum combination of one station having a cc=0.95 while a second station fulfills cc≥0.90 for at least one template of the same event.

We accept high similarity on only two stations (except for the early period, where only one is available)

here because of the relative sparsity of the station network, and to avoid missing events in down-times of stations. For example if an event just met the above criteria, but the closest or second closest station would not be working, the replacement station (third in distance) would most certainly have a lower cc because of the distance dependence of the cross correlation measure. We would then miss the event. Adding more stations to the matching criteria would increase this observational selection bias.

Note, that the applied criteria, using a relatively high cc threshold at several stations and the long time window including both P and S phases, are comparatively strict ([Uchida and Bürgmann, 2019](#); [Gao et al., 2021](#)). We decided not to include the inter-event distance as an additional constraint for co-location of the events, because the location uncertainty can be of the order of a few kilometers ([Münchmeyer et al., 2025](#)). This is significantly larger than most of the estimated source dimensions. In particular, deep and/or offshore seismicity and the comparatively sparse station geometry also complicate the otherwise often effective reduction of location errors by application of relative relocation methods.

In the resulting RE catalog, each new detection inherits the location of its template. Events which were already part of the Atacama catalog and which are grouped together by high cc values keep their original location.

The seismic moment is estimated from the magnitudes provided in the Atacama seismic catalog, which provides an equivalent to moment magnitude called MA. For newly detected repeaters, which are not contained in the original catalog, we compute the amplitude ratio of the detected event to the template event, and average over the available stations, as described in [Folesky et al. \(2025\)](#). Figure S3 shows the consistency of the newly estimated magnitudes with the Atacama catalog magnitudes.

For each event of a RE sequence, we can then estimate the slip by using the empirical slip-to-moment relation originally introduced by [Nadeau and Johnson \(1998\)](#). Note, that we have not corrected this slip relation for the local background slip rate. Hence, the computed slip values should be seen as a proxy for the true distribution rather than to be taken absolutely. This has been done similarly for other repeater catalogs, such as [Igarashi \(2020\)](#); [Folesky et al. \(2025\)](#). We have chosen this simple relation, as it is often used and easy to apply. The reader should be aware that for more accurate measures the background slip rates should be considered ([Chen et al., 2007](#)) and that multiple alternative/updated relations could be used to compute the slip (e.g. [Beeler et al., 2001](#); [Nadeau and McEvilly, 2004](#); [Khoshmanesh et al., 2015](#)). For example, by using the regional 6.7 cm/yr plate convergence velocity as normalization factor ([Chen et al., 2007](#)) the recurrence time to moment relation of our data set fits well to those of other regions (cf. Figure S9).

We additionally assign the tectonic class of the repeater location as specified in the Atacama seismic catalog to each RES. Possible labels are: interface (428), upper plane (384), lower plane (215), intraslab (50), upper

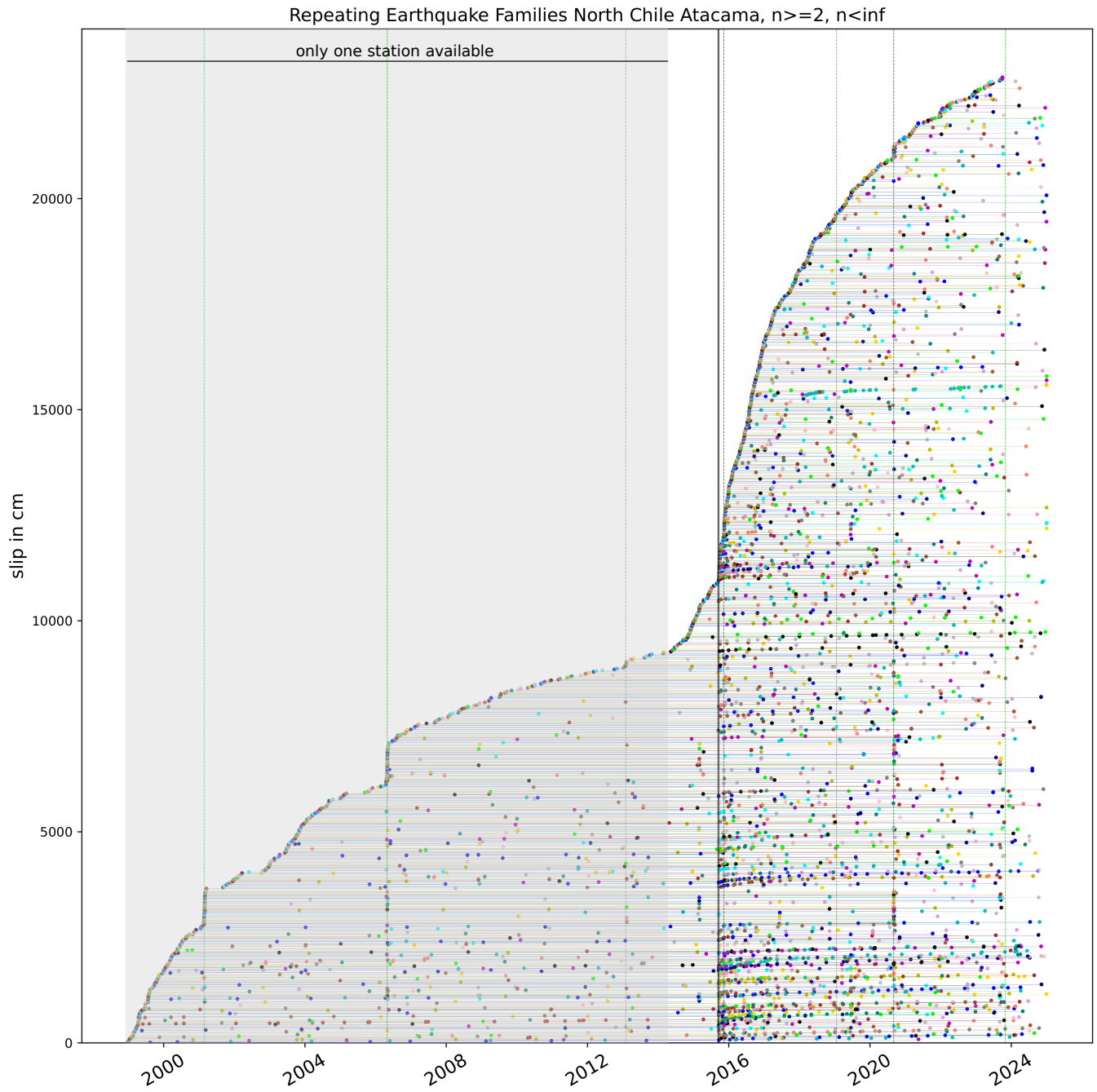


Figure 2 Slip vs. time for all 1142 repeater families reported in this work. Plotting order is chronological, starting with the series that has the very first event identified RE that belonged to any repeater group. The second series is the one containing the second identified RE, etc. For plotting only, each sequence is offset to the previous by 20cm slip. In this way the figure shows new RES (envelope) and recurrences of known groups (similar colored dots). The black vertical line denotes the occurrence time of the 2015 M_W 8.3 Illapel earthquake. Note its big influence on repeater occurrence rates, both, on existing series and new. Green dashed vertical lines denote occurrence times from selected large magnitude earthquakes ($M \geq 5.7+$) in the target region, taken from USGS earthquake catalog. Be aware that before 2014-05 (grey shaded area) REs are identified by one station only (IU.LCO), and that this limitation might have an influence on the apparent activity. In the supplement, similar figures sorted by RES event numbers are shown (Fig.S4-S8).

plate (40), mislocated (3), outer rise (12) or mineblast (8), where in brackets the number of RESs per category is given.

Finally, the repeater series are classified by their recurrence pattern as defined by Waldhauser and Schaff (2021) and as described in Folesky et al. (2025). The possible labels are: *qp* - quasi periodic(141), *bu* - burst(8), *dc* - decay(187), *rb* - repeated burst(17), and *ap* - aperi-

odic(88). Series may bear more than one recurrence type tag, when their behavior fits to more than one class. For example, a quasi periodic series may be affected by a large event occurrence and change its recurrence type from *qp* to *dc*. Eventually it may return to *qp* within the long observation interval of 26 years. Each recurrence curve was double-checked manually following the initial automated classifier to resolve the more complex

cases. Note, however, that the classification is based on rather arbitrary parameters and small shifts may lead to different type associations. A spatial distribution of the types is shown in Figure S10. For more details on the classification, see Folesky et al. (2025).

4 Results

We found 4,781 events in 1,142 RE sequences (RES) in the study region in the Atacama segment of the Chile subduction zone between 24.5°S and 30.5°S for the analyzed time period from late 1998 to the end of 2024. Their spatial distribution is shown in Figure 1, where the location of each RE family is represented by its geometric median. Their combined temporal occurrence history is shown in Figure 2. Repeaters are observed at the plate interface, but also in the continental crust of the upper plate, in the double seismic zone within the subducting slab, and at intermediate depth. The overall percentage of REs in the cataloged seismicity is $n_{RE}/n_{cat} = 2146/60,374 = 3.5\%$, where the newly detected REs are not considered. The new detections ($n=2635$) are split into $n=1031$ detected in the years 1998–2014 and $n=1604$ detected in the years covered by the Atacama catalog. This means $1604/(2146 + 1604) \approx 43\%$ of the repeaters would have been missed by “in catalog” template matching in that time window. This may be highly important when computing cumulative slip or slip rates. We found that several mining event clusters met our criteria for repeaters. The number of such mining events that formally classify as REs is 42, from which 16 were cataloged in the Atacama catalog. They are not included in the repeater catalog and the above event count, but we provide a list of them in a separate file (see Data and code availability section). The event count distributions of the RE families and their magnitude frequency distribution are shown in Figures 3 & 4, respectively. Most families are doublets and triplets ($n_{fam_{n=2}}=613$, $n_{fam_{n=3}}=173$), but there exist numerous larger families ($n_{fam_{n>3}}=356$) which are especially interesting for further analysis.

Exemplarily, waveforms for two repeating earthquake families, fam_{cID595} consisting of 14 events and fam_{cID154} consisting of 4 events, are illustrated in Figures 5 & 6, together with their median locations and estimated cumulative slip history.

The two series show very different rupture histories. Fam_{cID595} initiated shortly after the main shock of the 2015 $M_W 8.3$ Illapel earthquake. In its early phase, it exhibits short recurrence intervals which extend progressively with time and result in a temporal decay of the slip-rate (cf. Figures 5) until an approximately constant slip-rate is reached, which is still approximately ongoing. The Illapel megathrust event apparently initiated the series, modulated temporarily the stress field and induced time-dependent after slip in the area of the repeater asperity.

In contrast, fam_{cID154} was not affected by the Illapel mainshock due to its location further north. This group, however, shows clear co-occurrences of two of its four members with two $M 5.6+$ events, as shown in Figure 6C&D. Note, that without including the station

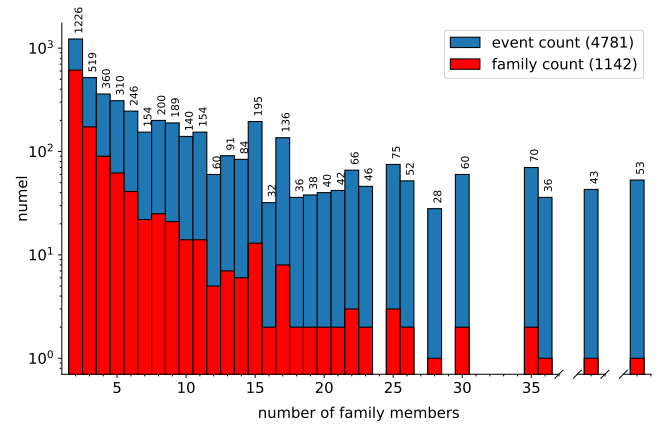


Figure 3 Histogram of number of individual RE events (blue) and number of RE families of a given family size (red). E.g., there exists one family (red bar count = 1) with 36 members (blue bar count = 36), but three families each with 25 members with a total of 75 events. Note the broken x-axis for better visualization.

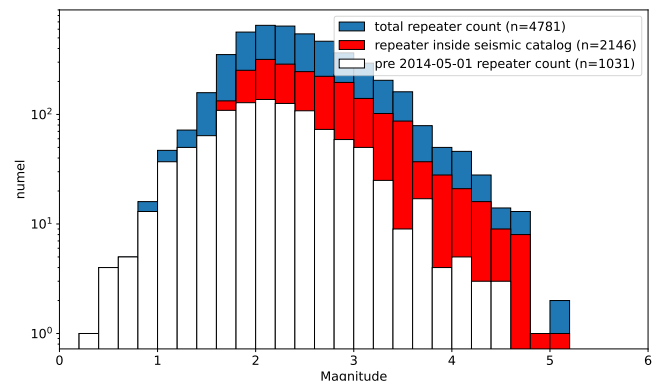


Figure 4 Magnitude frequency distribution of the repeater catalog. Blue bars indicate magnitude counts for the entire repeater catalog. Red bars show magnitude counts of repeaters that were already part of the seismic catalog. White bars depict magnitude counts of events that occurred before 2014-05-01, the date of the start of the seismic catalog.

LCO the first event of this series would have remained unidentified.

Fam_{cID595} was labeled as a decay type series and fam_{cID154} bears the label quasi periodic although it could alternatively have been labeled aperiodic.

The assigned parameters provide a means to find and extract more easily specific RE groups. For example, there exist several RE sequences that exhibit atypically high event counts. Figure S8 illustrates the 3 series that consist of more than 40 members. The computed cumulative slip of these groups would be considerably above the expected long term loading rates. Specific local features such as transient high fluid pressure or the stress redistribution effect of a nearby large earthquake could provide an explanation for the temporarily increased slip accumulation in regions of otherwise low loading rates. Alternatively, the multiplets may indicate the activation of adjacent rather than overlapping fault patches.

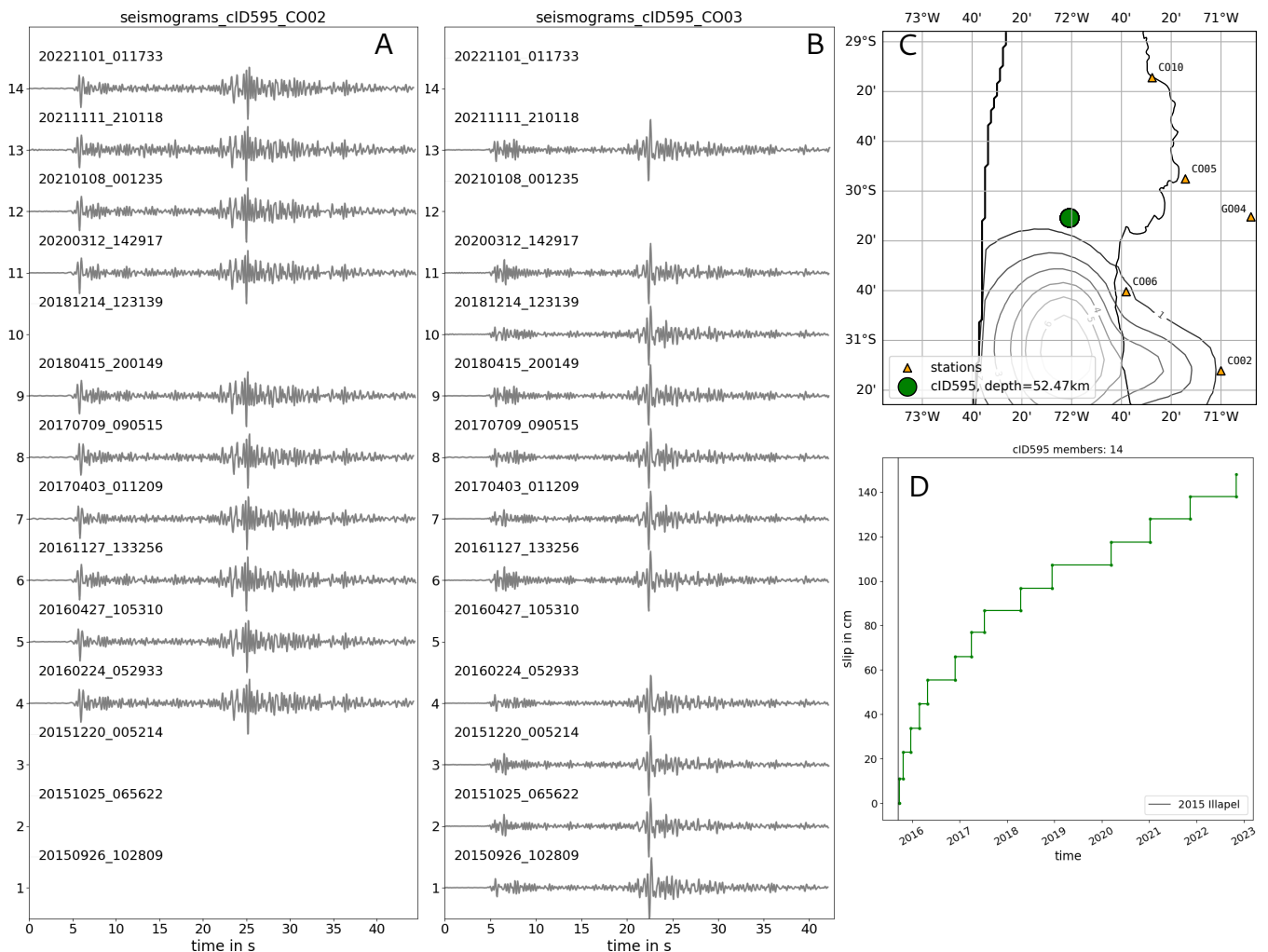


Figure 5 Repeating earthquake family 595. For this family, 14 members were detected. A and B show z-component velocity waveforms filtered between 1–4 Hz from stations CO02 and CO03, respectively. The time window starts five second before the p pick and spans about twice the Ts-Tp differential time. C shows the family location (slip contours by Ruiz et al. (2016)) and D displays slip vs. time.

Note the remarkable similarity between the events. The seismic activity of the family started just after the Illapel event, and it is continuous. The average slip-rate decreases rapidly (i.e., the inter-event waiting time increases) in the first three years after occurrence until it stabilizes onto a linear slope.

A more detailed analysis, involving careful relocation and individual source parameter estimation, would be necessary to better resolve the source processes of these event groups. This task is beyond the scope of this work. In a next step, we have used the new repeater catalog to compute a time resolved, first order slip-rate map of the plate interface for the entire study region, assuming that these repeater groups are indeed indicative for local slip at the plate interface, which we treat here as one single fault. First, we select RE sequences with a maximal distance of 15 km to the plate interface. For each RE sequence, the slip between each pair of subsequent events is divided by their inter-event time to estimate the slip-rate for the corresponding time period. These slip-rate values are assigned to each month between the first and last member of a series. In case of multiple events in a given month, the slip rates are averaged. Next, the monthly slip rates are averaged with those of other neighboring series on a regular spatial grid. The results can be displayed for a given time frame,

from one month to multiple years. Figure 7 shows the biyearly averaged slip-rates for the Atacama segment in north-central Chile for the years 2000 to 2024. It illustrates the large variability of slip in both space and time. In the years 2000–2007 some enhanced activity is imaged between 27°S and 28°S, but it is decaying in later years. In the region of the 2015 Illapel event, repeater activity is existent but low to moderate in the years before 2014/15. After the large megathrust event, afterslip and postseismic relaxation can be seen at least up to 2022. Only in 2024 the preseismic rates are reached again. Additionally, there appears to be some short term high rate activity indicated in the north of the target region in the subfigures of years 2018 and 2022 of Figure 7. Similar observations have been made for repeaters in the vicinity of large earthquakes in other world regions (e.g. Chen et al., 2010; Chalumeau et al., 2021; Waldhauser and Schaff, 2021; Folesky et al., 2025).

We plot the slip vs. time curves for all repeater families in Figure 2 as well as more detailed images in the

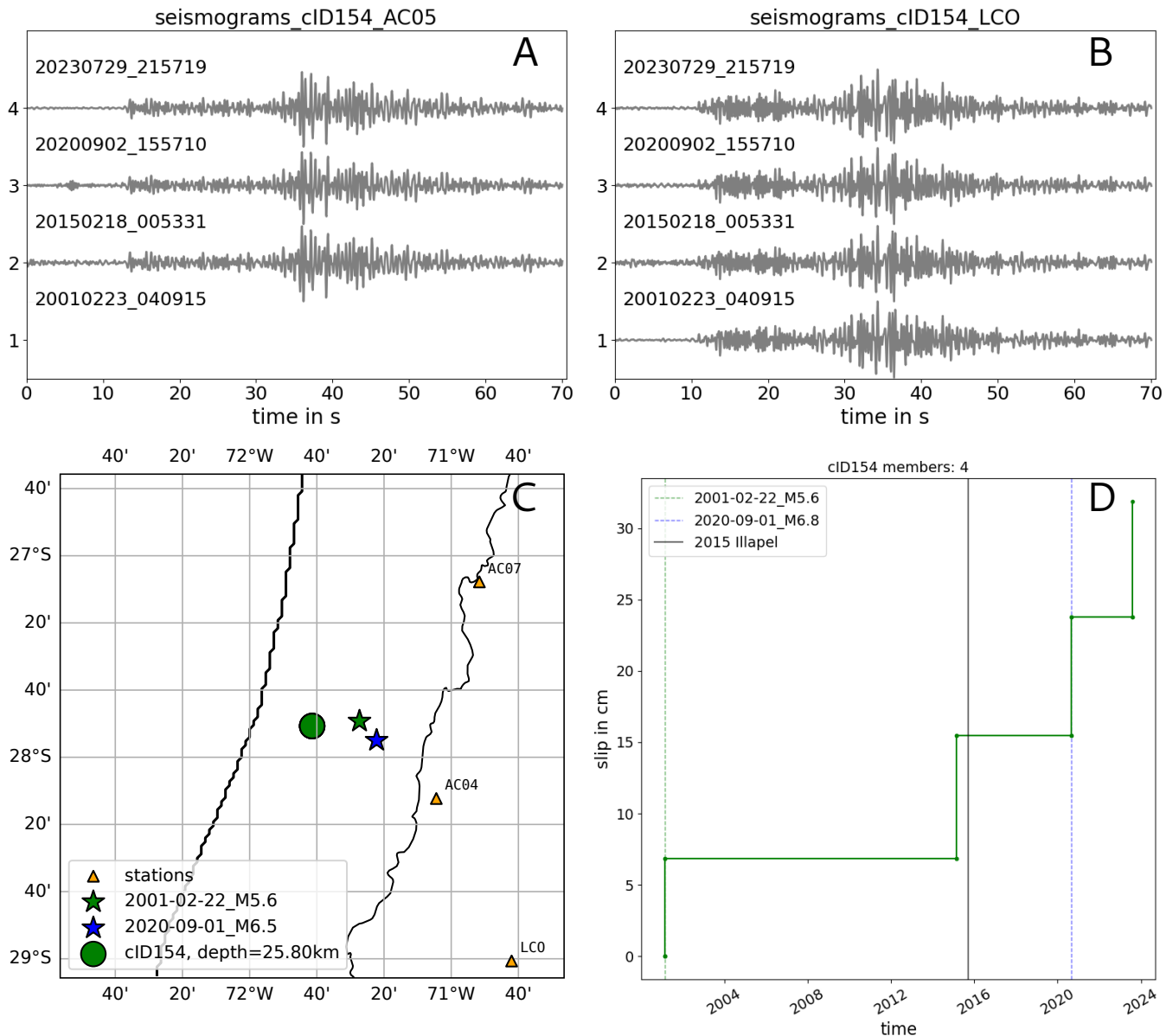


Figure 6 Repeating earthquake family 154. For this family, 4 members were detected. A and B show z-component velocity waveforms filtered between 1-4 Hz from stations AC05 and LCO, respectively. C shows the family location, where the green and blue stars show two large magnitude event locations in the direct vicinity of the event. Their occurrence times are shown in D as dashed colored lines. They coincide with the initiation of the series, and its second repeat. The Illapel earthquake, further south (occurrence time: black vertical line in D) did not impact this series.

electronic supplement (Fig. S4-S8) to illustrate the large variability of repeater recurrence variants. The importance of the 2015 M_W 8.3 Illapel earthquake and several other large magnitude events on the occurrence of the observed RE series in the region is clearly evident in these figures.

5 Conclusions

We report here on a repeating earthquake catalog for the Atacama segment of the subduction zone in north-central Chile between 24.5°S and 30.5°S in the time period from late 1998 to the end of 2024. The catalog comprises 4781 events grouped into 1142 repeater series. We use a template matching algorithm which scans the con-

tinuous seismic waveform data provided by the permanent networks of the region in order to identify repeating events. This computationally expensive approach significantly improves the completeness of the investigated repeater series, compared to waveform cross-correlation of only the earthquakes reported in the underlying seismicity catalog by Münchmeyer et al. (2025) which we find to contain about 60% of all identified repeaters.

In general, the repeater catalog describes a considerable spatial and temporal variety of recurrence behavior of repeater series. We observe repeaters mostly along the interface of the subducting Nazca slab, and much less for intraslab seismicity. Few intermediate depth repeaters are identified as well as only few re-

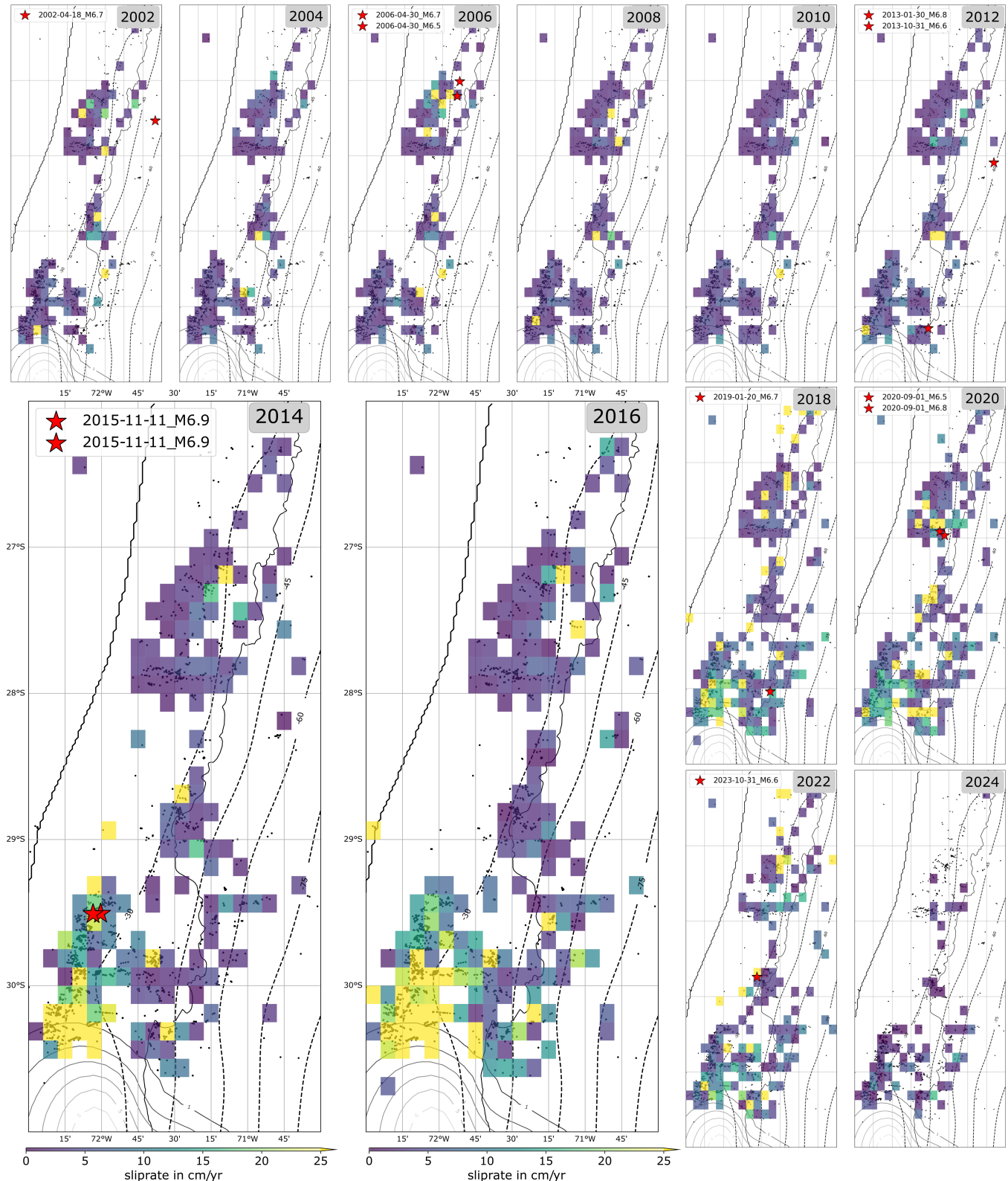


Figure 7 Biyearly averaged slip-rate maps for 2000-2024. The year is indicated in the upper right corner of each subplot. Slip-rates are averaged for all RES in a given cell over two years. No spatial smoothing is applied between cells. Highest slip-rates are found north of the $M_W 8.3$, 2015, Illapel event in the years 2015 to 2022. The coseismic slip contours are underlain (Ruiz et al., 2016). Black points are all RES. The enlarged maps show the years 2014-15 and 2016-17. The red stars indicate selected $M > 6$ event epicenters. The plate convergence rate is on average 6.7 cm/yr. Larger images of the individual maps are shown in the supplement Figures S11-S17.

peater sequences in the crust of the upper plate. REs at the interface indicate strong afterslip in the regions of the largest megathrust earthquake in the region, the

2015 $M_W 8.3$ Illapel event, but several series also react to some $M 5.7+$ events in their direct vicinity.

Based on the repeater catalog we compute a first time-

resolved map of the slip rates at the plate interface for the time period from 2000 to 2024. It shows strong segmentation of the Atacama Section of the Chilean subduction zone, with less activity in the north and more in the south. It also enables us to identify temporal variations, that are strongest in the region of the 2015 Illapel earthquakes but can be observed in other spots on a smaller scale, too.

The reported catalog lists all obtained repeating events and describes their associated repeater families, including a classification of their recurrence behavior type, their tectonic class and several parameters such as magnitudes, average locations, slip, observation period and coefficient of variation.

In the target region station availability increased significantly after 2014-05 from one to over 20 permanent stations. Therefore, we provide the results as a joint data set (1998-2024) and additionally only the part after 2014-05-01.

This work is intended to provide a valuable basis for future research on repeating earthquakes and helps to contribute to a better understanding of the dynamics of the entire subduction zone and the earthquake cycle of large events.

Acknowledgements

JF was funded by the German Science Foundation (DFG), project numbers FO 1325/3-1. We are grateful for suggestions by an anonymous reviewer and M.Radiguet.

Data and code availability

The repeater catalog is made available permanently at <https://doi.org/10.5281/zenodo.17276739>. It consists of the following files: 1) the list of repeating earthquakes with all additional parameters as computed in this study, 2) the list of mining events, that fulfill the repeater identification requirements but bear the label mining, and 3) the list of event pairs that have been used to construct the repeater groups including the station information and cross correlation values. File one is given in a post-2014 and in a combined version.

The Atacama seismic catalog ([Münchmeyer et al., 2025](#)) is available at <https://doi.org/10.5281/zenodo.15083298>.

The template matching code is available in static form at <https://doi.org/10.5880/fidgeo.2023.024> and in a maintained version under <https://github.com/RensHofman/SeismicMatch>.

Further processing and visualization was performed in python 3.7 using numpy ([Harris et al., 2020](#))v1.21.6, pandas ([pandas development team, 2020](#))v1.3.4, obspy ([Beyreuther et al., 2010](#))v1.2.2, cupy ([Okuta et al., 2017](#))v.11, matplotlib ([Hunter, 2007](#))v3.5.1 & cartopy ([Met Office, 2010-2015](#))v0.20.2..

Competing interests

The authors declare that they have no competing interests.

References

- Beeler, N., Lockner, D., and Hickman, S. A simple stick-slip and creep-slip model for repeating earthquakes and its implication for microearthquakes at Parkfield. *Bulletin of the Seismological Society of America*, 91(6):1797–1804, 2001. doi: [10.1785/0120000096](https://doi.org/10.1785/0120000096).
- Beyreuther, M., Barsch, R., Krischer, L., Megies, T., Behr, Y., and Wassermann, J. ObsPy: A Python toolbox for seismology. *Seismological Research Letters*, 81(3):530–533, 2010. doi: [10.1785/gssrl.81.3.530](https://doi.org/10.1785/gssrl.81.3.530).
- C. Seismic Network, Universidad de Chile, Red Sismologica Nacional, 1991. <https://www.fdsn.org/networks/detail/C/>.
- C1. Seismic Network, Universidad de Chile, Red Sismologica Nacional, 2012. doi: [10.7914/SN/C1](https://doi.org/10.7914/SN/C1).
- Chalumeau, C., Agurto-Detzel, H., De Barros, L., Charvis, P., Galve, A., Rietbroek, A., Alvarado, A., Hernandez, S., Beck, S., Font, Y., et al. Repeating earthquakes at the edge of the afterslip of the 2016 Ecuadorian MW7.8 Pedernales earthquake. *Journal of Geophysical Research: Solid Earth*, 126(5):e2021JB021746, 2021. doi: [10.1029/2021JB021746](https://doi.org/10.1029/2021JB021746).
- Chen, K. H., Nadeau, R. M., and Rau, R.-J. Towards a universal rule on the recurrence interval scaling of repeating earthquakes? *Geophysical Research Letters*, 34(16), 2007. doi: [10.1029/2007GL030554](https://doi.org/10.1029/2007GL030554).
- Chen, K. H., Bürgmann, R., Nadeau, R. M., Chen, T., and Lapusta, N. Postseismic variations in seismic moment and recurrence interval of repeating earthquakes. *Earth and Planetary Science Letters*, 299(1-2):118–125, 2010. doi: [10.1016/j.epsl.2010.08.027](https://doi.org/10.1016/j.epsl.2010.08.027).
- Folesky, J., Kummerow, J., and Hofman, L. J. A repeating earthquake catalog for Northern Chile. *Seismica*, 4(2), Aug. 2025. doi: [10.26443/seismica.v4i2.1578](https://doi.org/10.26443/seismica.v4i2.1578).
- Gao, D., Kao, H., and Wang, B. Misconception of waveform similarity in the identification of repeating earthquakes. *Geophysical Research Letters*, 48(13):e2021GL092815, 2021. doi: [10.1029/2021GL092815](https://doi.org/10.1029/2021GL092815).
- Harris, C. R., Millman, K. J., van der Walt, S. J., Gommers, R., Virtanen, P., Cournapeau, D., Wieser, E., Taylor, J., Berg, S., Smith, N. J., Kern, R., Picus, M., Hoyer, S., van Kerkwijk, M. H., Brett, M., Haldane, A., del Río, J. F., Wiebe, M., Peterson, P., Gérard-Marchant, P., Sheppard, K., Reddy, T., Weckesser, W., Abbasi, H., Gohlke, C., and Oliphant, T. E. Array programming with NumPy. *Nature*, 585(7825):357–362, Sept. 2020. doi: [10.1038/s41586-020-2649-2](https://doi.org/10.1038/s41586-020-2649-2).
- Hofman, L. J., Kummerow, J., Cesca, S., Group, A.-S.-D. W., et al. A new seismicity catalogue of the eastern Alps using the temporary Swath-D network. *Solid Earth*, 14(10):1053–1066, 2023. doi: [10.5194/se-14-1053-2023](https://doi.org/10.5194/se-14-1053-2023).
- Hunter, J. D. Matplotlib: A 2D graphics environment. *Computing in Science & Engineering*, 9(3):90–95, 2007. doi: [10.1109/MCSE.2007.55](https://doi.org/10.1109/MCSE.2007.55).
- Igarashi, T. Catalog of small repeating earthquakes for the Japanese Islands. *Earth, Planets and Space*, 72(1):1–8, 2020. doi: [10.1186/s40623-020-01205-2](https://doi.org/10.1186/s40623-020-01205-2).
- Igarashi, T., Matsuzawa, T., and Hasegawa, A. Repeating earthquakes and interplate aseismic slip in the northeastern Japan subduction zone. *Journal of Geophysical Research: Solid Earth*, 108(B5), 2003. doi: [10.1029/2002JB001920](https://doi.org/10.1029/2002JB001920).

IPOC. IPOC Seismic Network. Integrated Plate boundary Observatory Chile - IPOC, GFZ German Research Centre for Geosciences; Institut des Sciences de l'Univers-Centre National de la Recherche CNRS-INSU, Seismic Network, 2006. doi: 10.14470/PK615318.

IU. Albuquerque Seismological Laboratory/USGS, Global Seismograph Network (GSN - IRIS/USGS), 1988. doi: 10.7914/SN/IU.

Khoshmanesh, M., Shirzaei, M., and Nadeau, R. M. Time-dependent model of aseismic slip on the central San Andreas Fault from InSAR time series and repeating earthquakes. *Journal of Geophysical Research: Solid Earth*, 120(9):6658–6679, 2015. doi: 10.1002/2015JB012039.

Matsuzawa, T., Uchida, N., Igarashi, T., Okada, T., and Hasegawa, A. Repeating earthquakes and quasi-static slip on the plate boundary east off northern Honshu, Japan. *Earth, planets and space*, 56:803–811, 2004. doi: 10.1186/BF03353087.

Menke, W. Using waveform similarity to constrain earthquake locations. *Bulletin of the Seismological Society of America*, 89(4): 1143–1146, 1999. doi: 10.1785/BSSA0890041143.

Met Office. *Cartopy: a cartographic python library with a Matplotlib interface*. Exeter, Devon, 2010–2015. doi: 10.5281/zenodo.1182735. Available at <https://scitools.org.uk/cartopy>.

Münchmeyer, J., Molina-Ormazabal, D., Marsan, D., Langlais, M., Baez, J.-C., Heit, B., González-Vidal, D., Moreno, M., Tilmann, F., Lange, D., and Socquet, A. Characterizing the Atacama Segment of the Chile Subduction Margin (24°S–31°S) With >165,000 Earthquakes. *Journal of Geophysical Research: Solid Earth*, 130 (7):e2025JB031256, 2025. doi: 10.1029/2025JB031256.

Nadeau, R. M. and Johnson, L. R. Seismological studies at Parkfield VI: Moment release rates and estimates of source parameters for small repeating earthquakes. *Bulletin of the Seismological Society of America*, 88(3):790–814, 1998. doi: 10.1785/BSSA0880030790.

Nadeau, R. M. and McEvilly, T. V. Periodic pulsing of characteristic microearthquakes on the San Andreas fault. *Science*, 303(5655): 220–222, 2004. doi: 10.1126/science.1090353.

Okuta, R., Unno, Y., Nishino, D., Hido, S., and Loomis, C. CuPy: A NumPy-Compatible Library for NVIDIA GPU Calculations. In *Proceedings of Workshop on Machine Learning Systems (LearningSys) in The Thirty-first Annual Conference on Neural Information Processing Systems (NIPS)*, 2017. http://learningsys.org/nips17/assets/papers/paper_16.pdf.

pandas development team, T. pandas-dev/pandas: Pandas, Feb. 2020. doi: 10.5281/zenodo.3509134.

Ruiz, S., Klein, E., Del Campo, F., Rivera, E., Poli, P., Metois, M., Christophe, V., Baez, J. C., Vargas, G., Leyton, F., et al. The seismic sequence of the 16 September 2015 M w 8.3 Illapel, Chile, earthquake. *Seismological Research Letters*, 87(4):789–799, 2016. doi: 10.1785/0220150281.

Uchida, N. Detection of repeating earthquakes and their application in characterizing slow fault slip. *Progress in Earth and Planetary Science*, 6(1):1–21, 2019. doi: 10.1186/s40645-019-0284-z.

Uchida, N. and Bürgmann, R. Repeating earthquakes. *Annual Review of Earth and Planetary Sciences*, 47:305–332, 2019. doi: 10.1146/annurev-earth-053018-060119.

Waldhauser, F. and Schaff, D. P. A comprehensive search for repeating earthquakes in northern California: Implications for fault creep, slip rates, slip partitioning, and transient stress. *Journal of Geophysical Research: Solid Earth*, 126(11):e2021JB022495, 2021. doi: 10.1029/2021JB022495.

The article *A repeating earthquake catalog for the Atacama Segment in North Chile (24.5°S-30.5°S)* © 2026 by Jonas Folesky is licensed under CC BY 4.0.